

# Drag:on – A Virtual Reality Controller Providing Haptic Feedback Based on Drag and Weight Shift

André Zenner

German Research Center for Artificial Intelligence (DFKI)  
Saarland Informatics Campus  
Saarbrücken, Germany  
andre.zenner@dfki.de

Antonio Krüger

German Research Center for Artificial Intelligence (DFKI)  
Saarland Informatics Campus  
Saarbrücken, Germany  
krueger@dfki.de



**Figure 1:** The five states of our shape-changing haptic VR controller *Drag:on* investigated in our user study. a) shows the device state  $S_{closed}$  with minimal surface area. When increasing its surface area symmetrically as shown in b) ( $S_{half}$ ) and c) ( $S_{full}$ ), the controller adapts its drag and mass distribution to provide different haptic sensations during VR interaction. If opened asymmetrically on the d) left ( $S_{left}$ ) or e) right ( $S_{right}$ ) side, torque is induced when moving the controller.

## ABSTRACT

Standard controllers for virtual reality (VR) lack sophisticated means to convey a realistic, kinesthetic impression of size, resistance or inertia. We present the concept and implementation of *Drag:on*, an ungrounded shape-changing VR controller that provides dynamic passive haptic feedback based on drag, i.e. air resistance, and weight shift. *Drag:on* leverages the airflow occurring at the controller during interaction. By dynamically adjusting its surface area, the controller changes the drag and rotational inertia felt by the user. In a user study, we found that *Drag:on* can provide distinguishable levels of haptic feedback. Our prototype increases the haptic realism in VR compared to standard controllers and when rotated or swung improves the perception of virtual resistance. By this, *Drag:on* provides haptic feedback suitable for rendering

different virtual mechanical resistances, virtual gas streams, and virtual objects differing in scale, material and fill state.

## CCS CONCEPTS

• Human-centered computing → Virtual reality; Haptic devices; User studies.

## KEYWORDS

Haptic virtual reality controller, dynamic passive haptic feedback, shape-changing devices, air resistance feedback

## ACM Reference Format:

André Zenner and Antonio Krüger. 2019. Drag:on – A Virtual Reality Controller Providing Haptic Feedback Based on Drag and Weight Shift. In *CHI Conference on Human Factors in Computing Systems Proceedings (CHI 2019)*, May 4–9, 2019, Glasgow, Scotland UK. ACM, New York, NY, USA, 12 pages. <https://doi.org/10.1145/3290605.3300441>

## 1 INTRODUCTION

The core concept of virtual reality (VR) is the multisensory stimulation of the user, which makes it possible to feel present in immersive virtual environments (VEs). When experiencing the real world, humans rely heavily on their visual, auditory and haptic senses. While head-mounted displays (HMDs) and headphones enable users to perceive VEs visually and auditorily in immersive ways, VR systems today only provide very limited haptic impressions. Consumer

Permission to make digital or hard copies of all or part of this work for personal or classroom use is granted without fee provided that copies are not made or distributed for profit or commercial advantage and that copies bear this notice and the full citation on the first page. Copyrights for components of this work owned by others than the author(s) must be honored. Abstracting with credit is permitted. To copy otherwise, or republish, to post on servers or to redistribute to lists, requires prior specific permission and/or a fee. Request permissions from [permissions@acm.org](mailto:permissions@acm.org).  
*CHI 2019, May 4–9, 2019, Glasgow, Scotland UK*

© 2019 Copyright held by the owner/author(s). Publication rights licensed to ACM.

ACM ISBN 978-1-4503-5970-2/19/05...\$15.00

<https://doi.org/10.1145/3290605.3300441>

systems with lightweight hand-held controllers primarily offer vibrotactile feedback. These controllers, however, cannot provide different kinesthetic impressions such as the feeling of weight, resistance or inertia — haptic impressions that we expect and rely on when interacting with real environments.

Research in the past investigated different approaches to haptics in VR [20, 39, 47]. Recent research especially focused on techniques that can be integrated in hand-held controllers [12, 19, 40, 45, 47]. Many of them transform the controller such that users perceive different haptic impressions when interacting with it, e.g. by altering the mass distribution [23, 34, 47], the sensation at the fingertip [4, 45] or a physical connection between two controllers [40].

In this paper, we propose a novel concept for providing haptics to VR, introducing a combination of air resistance and weight shift as a means of generating haptic feedback. We present a novel shape-changing VR controller called *Drag:on* which leverages the airflow that occurs at the controller during VR interaction to provide a range of different haptic sensations. For this, *Drag:on* can self-transform while the user interacts in VR, to increase or decrease its surface area and to adapt its mass distribution. The controller provides dynamic passive haptic feedback [47], i.e. it uses actuators only to change the physical configuration of the device. By this, the device adapts to the virtual interaction and changes how it feels when moved through the air.

We introduce the underlying haptic feedback concept and our low-cost and mechanically simple prototype. Further, we present a user evaluation in which we studied how *Drag:on*'s haptic feedback can enhance the perception of virtual interactions in five VR scenarios. Our main contributions are:

- (1) The introduction of a novel concept of shape-changing VR controllers that provide dynamic passive haptic feedback based on air resistance and weight shift.
- (2) Our *Drag:on* prototype — the implementation of this shape-changing VR controller concept.
- (3) An evaluation comprising five VR scenarios, in which we study how users perceive *Drag:on*'s haptic feedback and how it compares to the haptics provided by an equivalent passive prop, and by state-of-the-art HTC Vive controllers [13].
- (4) Basic recommendations for the application of drag and weight-shift-based controllers such as *Drag:on* and the design of suitable VR experiences.

In the following sections we review related work, introduce the concept and implementation of *Drag:on*, and present our user study. We then discuss our findings and potential application areas, and reflect on future research directions.

## 2 RELATED WORK

This section briefly reviews approaches to haptics in VR, haptic VR controllers and air-based haptic feedback concepts.

### Approaches to Haptics in Virtual Reality

Haptic feedback concepts for VR can be categorized into active [39], passive [20], and mixed haptics [47]. In active approaches, computer-controlled actuators exert forces on the user during operation [39], e.g. through grounded haptic devices [27, 44], lightweight vibrotactile actuators [10], actuated pin arrays [4, 36], skin stretch mechanisms [29], body-worn electrical muscle stimulators [25, 26], or glove or exoskeleton-based systems [5, 11, 18]. While providing flexible feedback, a major limitation of many active approaches is their complexity, limited mobility or limited workspace. Passive haptic feedback (abbreviated *PHF* in the following), in contrast, does not involve any actuation to provide haptic impressions [20]. Instead, physical props in the real environment provide tangibility to virtual objects [35]. *PHF* is a low-complexity approach that can provide highly realistic haptic feedback when suitable props are provided. Being passive, however, it suffers from its general inflexibility.

To combine the strengths of active and passive haptics, researchers presented several mixed approaches. Cheng et al. [6, 7, 9] explored how actuators can be substituted by human actuation. Techniques like robotic graphics [2, 28, 43] leverage robotic actuation to present passive props to the VR user. Dynamic passive haptic feedback (abbreviated *DPHF* in the following) is another class of mixed haptics [47]. It is of crucial relevance for our work, as the prototype we present falls into this class of haptic devices for VR. *DPHF* devices are props equipped with actuators. Unlike traditional active haptic devices, however, the actuators are not used to actively render forces on the user, but to transform the prop itself in order to change how it feels. This enables a single prop to provide different passive haptic impressions before and after transformations, i.e. the prop physically adjusts to virtual objects and interactions.

Besides these approaches, techniques exist that heavily rely on visualization. In pseudo-haptics [14, 30], visual feedback is used to trigger haptic perceptions. Other concepts like redirected touching [22] and haptic retargeting [3, 8] make use of the visual dominance effect [17] by warping the virtual space or the user's hand to modify how users approach and touch physical props.

### Haptic Controllers for Virtual Reality

While expensive large-scale haptic interfaces with limited workspace are inappropriate in many everyday contexts, hand-held ungrounded VR controllers represent a practical compromise. Consumer devices today, like the HTC Vive

controllers [13], however, only provide very limited vibrotactile stimuli and always feel very lightweight. As such they are unable to render kinesthetic effects, e.g. virtual weight, resistance or inertia, in a realistic way. Recent research investigated how VR controllers can provide more realistic and immersive haptic feedback, while still being ungrounded. Whitmire et al.’s *Haptic Revolver* [45], for example, provides sensations at the fingertip by rotating a wheel carrying texture samples or interactive elements underneath the user’s index finger. Benko et al.’s [4] haptic controllers use a tiltable platform and an actuated pin array underneath the finger pad to convey the height, orientation, texture and shape of virtual surfaces. Choi et al. explored several ways to provide realistic haptics for touching, grasping, lifting and pressing virtual objects with *Wolverine* [11], *Gravity* [10] and *CLAW* [12]. Other controllers provide kinesthetic perceptions, like Zenner and Krüger’s weight-shifting VR controller *Shifty* [47], or Shigeyama et al.’s *Transcalibur* [34]. These controllers can render impressions of different virtual weights, sizes and shapes. Krekhov et al. [23] explored how such controllers can enhance player experiences in games. Apart from individual controllers, the *Haptic Links* by Strasnick et al. [40] connect two commodity VR controllers to enhance the haptics of two-handed interactions.

With *Drag:on*, we introduce the first *DPHF* controller that combines inertial adjustments with an intentional utilization of air resistance to produce kinesthetic sensations.

### Air-Based Haptic Feedback

A variety of approaches to air-based haptic feedback exist. The *AIREAL* [38], for example, shoots air vortices onto the user’s skin to produce tactile sensations. Romano and Kuchenbecker’s *AirWand* [32] produces kinesthetic haptic feedback based on air jet actuation. Rietzler et al. presented *VaiR* [31], a head-worn device for haptic airflow simulation. Other devices provide ungrounded force feedback through propeller propulsion used to generate thrust. Examples are Heo et al.’s [19] VR controller *Thor’s Hammer*, Je et al.’s [21] *Wind-Blaster* and Sasaki et al.’s [33] *LevioPole*.

Most related to our work is the concept investigated by Suzuki et al. [41, 42]. In their air jet driven system, users carry paddle-like objects, called air receivers. Nozzles at the location of virtual objects in the real environment release air streams when the paddle makes contact with a virtual object. Carrying the air receiver, the user feels the impacting air on the receiver as a soft contact force.

In contrast to our approach, however, existing air-based haptic feedback typically relies on powered propellers with high energy requirements or air jet actuation, requiring compressed air or air compressors to render forces. Our approach works without any of these, leveraging solely the airflow that occurs at the controller during VR interactions.

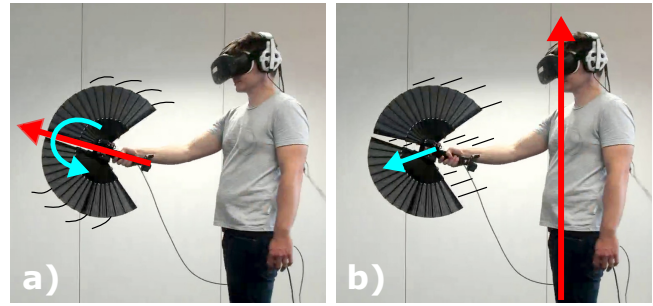


**Figure 2: The two investigated types of interaction with the movement direction (blue), the rotational axis (red) and the motion (black lines) highlighted. a) rotational movements (rolling the controller) and b) translational movements (swinging the controller).**

### 3 DRAG:ON – CONCEPT & IMPLEMENTATION

We introduce the concept of a shape-changing VR controller providing haptic feedback based on drag and inertia. With *Drag:on* we further present a first implementation thereof.

#### Haptic Feedback Concept

During many VR interactions, users swing, drag, throw or rotate virtual objects. In this context, rotational and translational motions of the controller (see Figure 2) are central. During such motions, an air stream forms at the device as the user pushes its resisting surface through the air.

The central idea underlying *Drag:on*’s *DPHF* is to adjust this surface area to produce different sensations of resistance when the controller is moved. Instead of simulating constant forces in a 1-to-1 manner, *Drag:on* leverages the motions of the user to provide resistance impressions that vary with velocity. Through immersive visualizations, the dominant impact of vision is used to bridge visual-haptic mismatches.

As shape-changing objects are well suited to complement the simulation of virtual objects [1], our controller transforms its shape to adjust its surface area at runtime. Depending on the implementation of the shape change, this entails secondary physical effects. To additionally make use of such, we opted for a design with foldable surfaces, i.e. fans, a form factor that has also been focus of research on foldable displays [24]. Our decision was based on two main considerations: 1) a fan-based design is mechanically simple, low-cost and easy to replicate, and 2) in addition to drag, it allows to leverage inertial changes, which was shown to be suitable for providing kinesthetic haptics in VR [16, 34, 47]. In our design, surface area is increased or decreased (Figure 1, a to c) by opening or closing two fans symmetrically on the left and right side of the controller. Additionally, our device can control the surface areas on both sides individually. Increasing the area only on one side of the device (Figure 1, d

and e) can induce torque. This torque rotates the controller in the user's wrist during motion and allows for rendering of asymmetric forces and differences in resistance.

Apart from drag, also the mass distribution of the object changes when opening or closing the fans, affecting the inertial response of the controller when rolling or swinging it. By opening the fans as shown in Figure 2 a), the moment of inertia  $I_{roll}$ , i.e. the rotational resistance when *rolling* the device about the longitudinal axis (indicated in red), increases as mass is moved away from the axis. This supports and amplifies the resistance feedback felt when rolling the controller with the wrist, in addition to the increased drag.

In contrast, when considering *swinging* the controller as shown in Figure 2 b), opened fans lead to mass being moved towards the swing-axis (indicated in red) passing through the user's shoulder. This reduces the corresponding rotational inertia  $I_{swing}$  and acts against our intended effect of increased resistance. It is not a practical limitation, though, as the relative change of  $I_{swing}$  when opening or closing the fans is much lower than the relative change of  $I_{roll}$ . As a simplifying assumption, we thus regard swinging the controller as translation in the following.

Finally, a shape change of the controller will also affect the drag coefficient of the device. In the presented implementation, opening the fans leads to reduced rigidity of the structure, which in turn leads to the controller bending in the airflow at higher motion speeds. While such bent shapes make the device more aerodynamic, the increase in surface area which is caused by the shape change remains the factor dominating the felt drag force in our design. Our evaluation will show that in practice, the drag feedback of our controller can produce the desired impressions despite these two counteracting effects.

Assuming a device with two adjusting fans, such as our prototype, the physical state of the device can be described by a tuple  $S = (open_{left}, open_{right})$ , given by the percentage of opening of the left and right fan. While such a device can take any state  $S \in [0, 100] \times [0, 100]$ , we focus our investigation on the five states defined in Table 1 and shown in Figure 1.

### Implementation of the Drag:on VR controller

In the following we present *Drag:on*: the simple, low-cost and easily reproducible implementation we used for studying the presented concept. Our device is not a definitive implementation, but rather one of many imaginable designs.

**Hardware.** The 3D rendering in Figure 3 shows the main components of the *Drag:on* device. The controller consists of a wooden base with a screwed-on custom-designed 3D-printed mount to attach the HTC Vive tracker. In addition, a 3D-printed grip holds a small pushbutton attached with a rubber band. The location of this button can be adjusted

**Table 1: *Drag:on* Prototype — Investigated States**

State	open <sub>left</sub> (%)	open <sub>right</sub> (%)	Area	Figure 1
$S_{closed}$	0	0	$320cm^2$	a)
$S_{half}$	50	50	$1320cm^2$	b)
$S_{full}$	100	100	$2400cm^2$	c)
$S_{left}$	100	0	$1410cm^2$	d)
$S_{right}$	0	100	$1250cm^2$	e)

to account for the handedness of the user. The actuation mechanism depicted in Figure 4 b) is located at the top end of the controller. On both sides of the controller, we fixed an MG996R servo motor using custom 3D-printed parts. Each servo actuates a 3D-printed arm attached to the topmost layer of a commercially available flamenco hand fan. The fans are 31cm long and made out of wood and fabric, as can be seen in Figure 1. The bottommost layer of the fan is rigidly attached to a 3D-printed support structure, pointing away from the user. By actuating the servo, the arm opens or closes the fan. Figure 4 b) shows a servo and an actuated arm opening a fan. To allow for unconstrained movements, the maximum opening angle of the right fan is slightly limited to leave enough space for the user's arm (see Table 2). In order to ensure comfortable interaction with the device, we designed the prototype to concentrate its mass close to the user's hand to minimize its overall moment of inertia.

Figure 4 a) shows the final prototype with its main system components. The device is connected to a controller box containing an Arduino Nano microcontroller and the necessary circuits. An external power adapter connects to this box to provide 7.6V to the motors. The Arduino interfaces with the PC via USB serial communication (115200 baud). Table 2 summarizes the technical data of the *Drag:on* prototype with the HTC Vive tracker attached. The surface area referred to in Table 1 and Table 2 is the area of its orthographic projection on a plane parallel to the fans, i.e. the area visible in Figure 1.

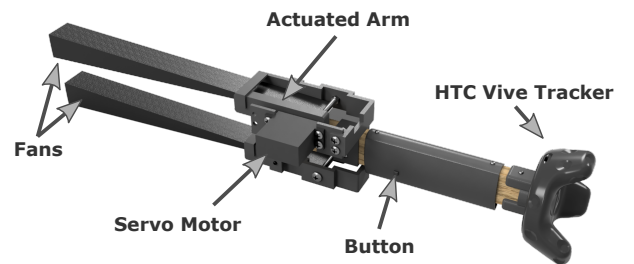


**Figure 3: 3D rendering of the *Drag:on* prototype.**



**Table 2: *Drag:on* Prototype – Technical Data**

Fan Angle	min.	5°
	max. left	152.5°
	max. right	132.5°
Area	min. ( $S_{closed}$ )	320cm <sup>2</sup>
	max. ( $S_{full}$ )	2400cm <sup>2</sup>
Time ( $S_{closed} \rightarrow S_{full}$ )	total	570ms
Power Consumption	idle	0.23W
	peak	6.84W
Length	fan	31cm
	total	54cm
Weight	fans	2 × 75g
	total	598g

As Table 2 shows, *Drag:on* can increase its surface area by up to  $\frac{A(S_{full}) - A(S_{closed})}{A(S_{closed})} = \frac{2400cm^2 - 320cm^2}{320cm^2} = 650\%$  in 570ms.

**Software.** The software stack of *Drag:on* involves two central components, depicted in green in the architecture overview in Figure 5. The C++ software controlling the device runs on the Arduino Nano. It forwards button state changes to the VR system and controls the servo motors upon reception of transformation commands. The Arduino uses a simple custom protocol to communicate with the VR system on the PC via USB serial connection. The second main component is the C# interface script for the Unity 3D engine. This script handles serial communication with the controller and implements convenient functions to control the state of the device. With these functions, the VE logic can send transformation commands to the *Drag:on* and receive button state changes.

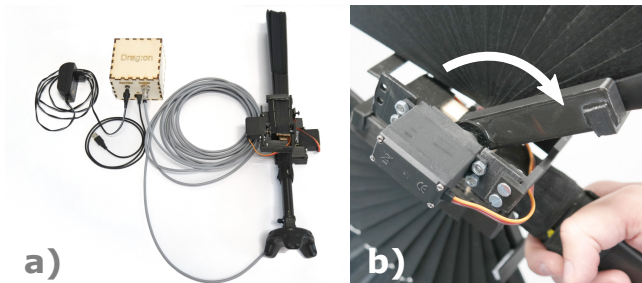


**Figure 4:** a) *Drag:on* system components. The *Drag:on* is connected with a long cable to a box holding the microcontroller and circuits. The box connects to the PC via USB. Motor power is provided by an external power adapter. b) a servo motor and connected arm opening a fan.

## 4 EVALUATION

We conducted a user study with  $N = 18$  (14 m, 4 f) volunteer participants aged between 21 and 33 years ( $Mdn = 27$ ,  $SD = 3$ ). All had normal or corrected-to-normal vision and 15 were right-handed. In 2 parts, we studied how a haptic VR controller providing combined drag and inertial feedback can enhance the user's perception of VEs.

The first part investigated how the *DPHF* of our controller is perceived in three different interactive VR scenarios. We compared different states of *Drag:on* to test if they can provide distinguishable levels of haptic feedback.

The second part studied the two types of interaction introduced in Figure 2, i.e. rotating and translating the controller, in two additional VR scenarios individually. Here, in addition to comparing different *Drag:on* states, we compared the *DPHF* of *Drag:on* to a *PHF* baseline and the vibrotactile feedback of standard HTC *VIVE* controllers.

The experiment was approved by the ethical review board of our faculty. It took place in a quiet lab environment and was carried out with our *Drag:on* prototype and an HTC Vive HMD, trackers and controllers; it was implemented with the Unity 3D engine. Participants stood in the center of the tracking area and had enough space to freely swing the controller. To dampen the sound of the servos, participants wore over-ear headphones with which they could hear the interactions and background sounds of the VE. To further exclude effects due to users perceiving servo noise or vibrations, we implemented an obfuscation mechanism to create random transformation noise each time *Drag:on* was supposed to change state. Whenever instructed to transform to a target state  $S$ , our controller first transformed to a random state  $S' \in [0, 100] \times [0, 100]$  before transforming to  $S$ . This effectively doubled the transformation time to up to 1140ms. In the study, however, this did not introduce significant delays as *Drag:on* only transformed in between user interactions.

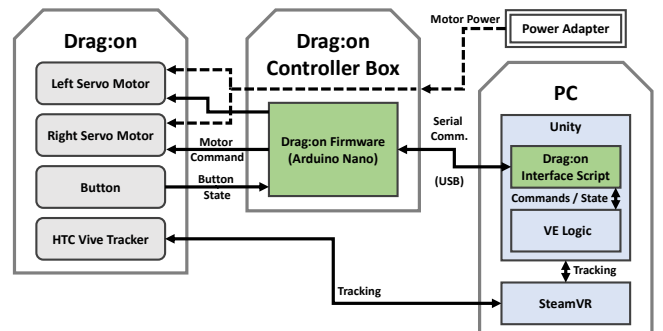


**Figure 5:** Overview of the software architecture of the *Drag:on* system. Sensors and actuators are colored in gray, software in blue, and the two main software components of *Drag:on* are highlighted in green.

## Experiment Procedure & Design

Before starting, participants were briefed by reading through a prepared document explaining the five scenarios of the study. They were intentionally not informed about the controllers interacted with and the *Drag:on* prototype was hidden from them until the end of the study. At the beginning of each scenario, participants could become familiar with the interaction and their task by performing a short training trial. We recorded their responses only after completion of the training trial. Upon completion of the last scenario, participants filled in the post-study questionnaires (SUS presence questionnaire [37], demographics and additional questions). The experiment ended with a short verbal debriefing and took ca. 95min per participant.

The study was designed as a within-subjects experiment. The order of scenarios in part 1 (*Scale*, *Material*, *Flow*) was counterbalanced by a 6x3 Williams design latin square (LS) [46], with the 9 trials in each scenario counterbalanced by a 18x9 LS. In part 2, 9 participants experienced the *Wagon* scenario after *Ratchet*, while for all others, this was reversed. The order of the 3 haptic conditions (*DPHF*, *PHF*, *VIVE*) tested in *Wagon* and *Ratchet* was counterbalanced by a 6x3 LS. Within each haptic condition, participants performed 9 trials (3 levels of feedback, each 3x), counterbalanced by a 18x9 LS.

### Part 1 – Comparing *Drag:on* States

The first part of the study compared the *Drag:on* states introduced in Table 1 in the three VR scenarios *Scale*, *Material* and *Flow*. In all these scenarios, participants were immersed in a virtual factory environment, holding the *Drag:on* prototype in their dominant hand and a secondary HTC Vive controller in their other hand. When a trial started, *Drag:on* transformed to the state associated with that trial (independent variable), with active obfuscation. *Drag:on* then remained in this state until the beginning of the next trial. In each trial, participants interacted with a virtual object (*Scale*, *Material*) or environment (*Flow*). The task of the participants in each scenario was to freely explore the haptic response of the object in their hand (*Scale*, *Material*) or the environment (*Flow*) to get a feel for it. They were free to do so by swinging the controller (in all 3 scenarios) or rotating it (only in *Scale* and *Material*). Their task was then to adjust the VR visualization of the virtual object or environment until it matched their haptic impression best. For this, in all three scenarios, a simple user interface (UI) was displayed on the secondary controller that allowed participants to adapt the visualization of the objects or environment interacted with. By pressing a button on the controller, participants could record their best-matching configurations (dependent variables).

**Scenario 1 – *Scale*.** The *Scale* scenario (**S**) compared the states  $S_{closed}$ ,  $S_{half}$  and  $S_{full}$ , and investigated our hypothesis:

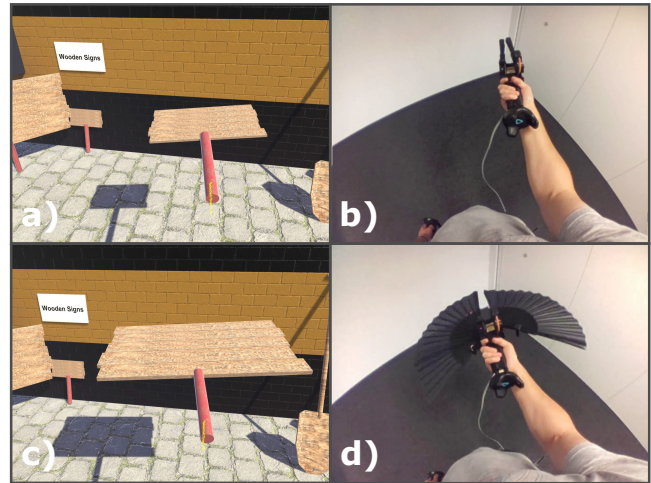


**Figure 6: *Scale* scenario:** a) the avg. scale (1.33) associated with b) the state  $S_{closed}$  is significantly smaller than c) the avg. scale (2.38) associated with d)  $S_{full}$ .

→ **H-S:** Users associate different *Drag:on* states with different virtual object sizes.

For this, participants interacted with a virtual wooden sign as shown in Figure 6. With the UI on the secondary controller, they could scale the sign up or down in the scaling range [1, 3], and record their selected best-matching scale.

**Scenario 2 – *Material*.** The *Material* scenario (**M**) compared  $S_{closed}$ ,  $S_{half}$  and  $S_{full}$  to test our hypothesis:

→ **H-M:** Users associate different *Drag:on* states with different virtual object materials.

Participants interacted with a virtual shovel as shown in Figure 7 a) and could change its material. Using the UI on the secondary controller, they could select and record their best-matching material from a set of three materials that visually implied different weights (lightweight plastic, medium-heavy wood, heavy metal).

**Scenario 3 – *Flow*.** The *Flow* scenario (**F**) explored how asymmetric drag-based haptics, especially in comparison to symmetric feedback, can enhance the perception of environmental elements like virtual gas flows. For this, we explored  $S_{left}$ ,  $S_{full}$  and  $S_{right}$  to test hypothesis:

→ **H-F:** Users associate different *Drag:on* states with different virtual gas flow distributions.

Participants interacted with a virtual paddle and faced an upper and lower gas stream, released through two pipes in front, as shown in Figure 8 a) and c). Their task was to swing the paddle horizontally through both gas streams towards the pipes (as illustrated by the arrow) to feel which of the streams is stronger, or if both are equally strong. Using the UI on the secondary controller, they could adjust the visualization

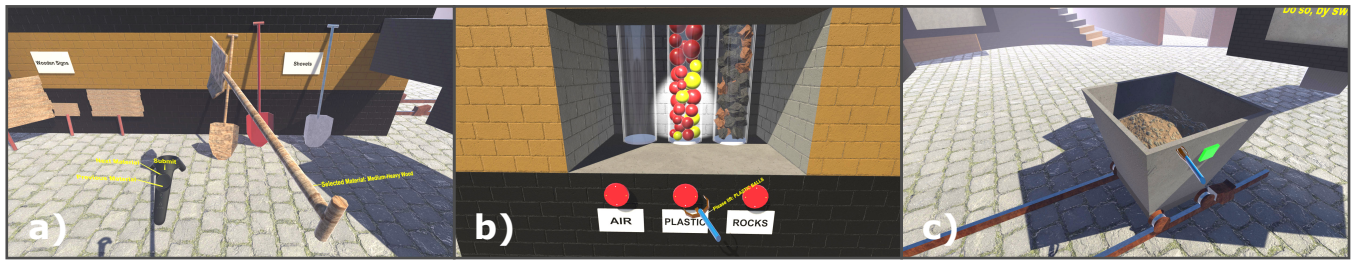


Figure 7: Participant views of the *Material*, *Ratchet* and *Wagon* scenarios. The participant a) selected a wooden *Material* for the shovel, b) is supposed to lift the plastic balls with the corresponding *Ratchet* and c) is about to move a half-filled *Wagon*.

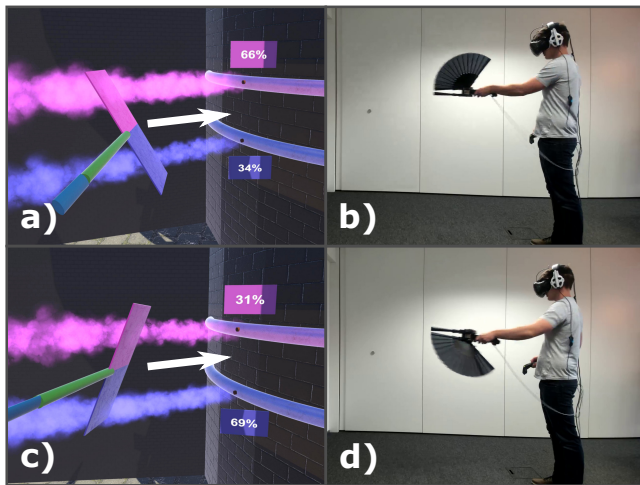


Figure 8: *Flow* scenario: a) the avg. relative upper gas flow (66%) associated with b)  $S_{right}$  is significantly stronger than c) the avg. relative upper flow (31%) associated with d)  $S_{left}$ .

of the streams and configure the relative stream strengths that they perceived as best-matching. For this, they could distribute a total power of 100% between the two streams. The relative upper gas flow strength of their selected best-matching configuration was recorded. We accounted for the handedness of participants by adapting the VE accordingly.

### Part 1 – Findings

We investigate the effect of the tested *Drag:on* states on the dependent variables of each scenario. For multiple comparisons, we performed non-parametric Friedman tests with pairwise post-hoc Wilcoxon signed-rank tests and applied a Bonferroni-Holm correction. Significant results of pairwise tests are indicated in the referenced charts ( $\alpha = .05$ ).

**Results.** Figure 9 shows the main results of the *Scale*, *Material* and *Flow* scenarios. Friedman tests found significant effects of *Drag:on* state on perceived object scale ( $\chi^2(2) = 32.11, p < .001$ ), and on perceived relative upper gas flow strength ( $\chi^2(2) = 36, p < .001$ ). Post-hoc analysis revealed a

significant difference in mean perceived object scale and upper gas flow strength for all pairwise comparisons of  $S_{closed}$ ,  $S_{half}$  and  $S_{full}$  in *Scale*, and of  $S_{left}$ ,  $S_{full}$  and  $S_{right}$  in *Flow* (all  $p < .001$ ). To evaluate the *Material* scenario, we computed the average probability of selecting a material as “best-matching” for each state and tested within each state for differences, as well as across states individually for each material. Friedman tests confirmed material probabilities to differ significantly within each state, as well as across states (all  $p \leq .009$ ). The probabilities and the results of the pairwise comparisons can be seen in the second chart in Figure 9.

**Discussion.** The results show that the haptic responses of the tested *Drag:on* states are distinguishable. *Drag:on* can successfully convey different object scales (here, of wooden signs – as illustrated in Figure 6) and the (dis)equilibrium of environmental effects like gas streams, given corresponding visual feedback. The comparison of  $S_{left}$ ,  $S_{right}$  and  $S_{full}$  shown in Figure 9 suggests that asymmetric states are suitable to convey relative resistance differences, especially in conjunction with symmetric states representing the absence of such. Our findings thus confirm **H-S** and **H-F**. Concerning material perceptions, with each of the tested *Drag:on* states, a different material was associated most often. The results indicate that  $S_{closed}$  is suitable to convey relatively lightweight materials like plastic,  $S_{full}$  is associated with rather heavy materials like wood or metal, and  $S_{half}$  can be used to render materials of intermediate weight (like plastic or wood). Comparing, for example, the results for  $S_{closed}$  and  $S_{full}$ , it can be seen that different states are indeed associated with different materials – confirming **H-M**.

### Part 2 – Comparing Haptic Feedback Techniques

The second part of our study investigated rotational (*Ratchet* scenario) and translational motions (*Wagon* scenario).

**Scenario 4 – Ratchet.** The *Ratchet* scenario studied how *Drag:on* can render mechanical resistance felt when turning ratchets. Participants stood in front of the interaction panel shown in Figure 7 b), facing three glass containers filled with



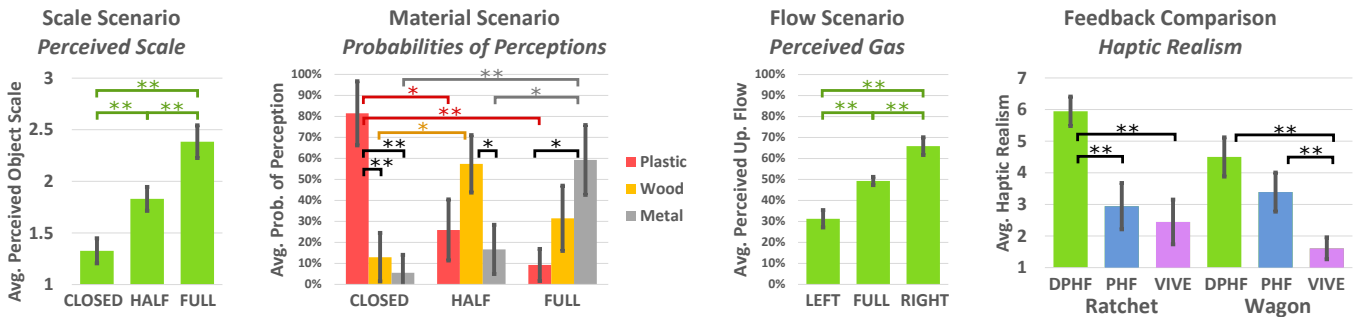


**Figure 9: From left to right: Scale chart plotting perceived virtual object scale. Material chart showing perception probabilities for the different materials. Flow chart illustrating perceived relative strength of the upper gas stream. Tested *Drag:on* states on the x-axis. The rightmost chart shows the haptic realism experienced in the DPHF, PHF and VIVE conditions in part 2 of our study. Brackets indicate statistically significant differences ( $p < .05$  (\*);  $p < .01$  (\*\*)). Error bars show 95% confidence intervals.**

air, plastic balls, and rocks. By turning the ratchet beneath a container with a rotational movement as shown in Figure 2 a), the corresponding content could be lifted up. The task of the participants was to lift each material three times and the material to lift next was indicated by a spotlight.

**Scenario 5 – Wagon.** The *Wagon* scenario investigated how *Drag:on* can render the weight felt when moving wagons in the VE. Here, participants had to move a virtual wagon as shown in Figure 7 c) along rails from right to left and back again by grasping, swinging (as shown in Figure 2 b) and releasing it with the controller. The wagon was visually either empty, half-filled, or completely filled with sand, and each fill state was experienced three times.

**Scenario 4 & Scenario 5.** Both scenarios compared the haptic perception of  $S_{closed}$ ,  $S_{half}$  and  $S_{full}$  as in part 1, and additionally compared *Drag:on*'s DPHF to a PHF baseline and the vibrotactile feedback of HTC Vive controllers. Each of the scenarios was experienced once with each haptic technique (DPHF, PHF, VIVE). In DPHF conditions, the different ratchets and fill states of the wagons were mapped to the tested states (air/empty  $\rightarrow S_{closed}$ , plastic/half-filled  $\rightarrow S_{half}$ , rocks/full  $\rightarrow S_{full}$ ) and *Drag:on* transformed to them when grasping the ratchet or wagon. In PHF conditions, participants also interacted with *Drag:on*, which here only transformed for obfuscation and always returned to  $S_{closed}$  for each ratchet and wagon – providing the feedback of an equivalent *passive* prop during interaction. In VIVE conditions, users interacted with an HTC Vive controller instead of *Drag:on*, providing different vibration patterns, implemented with the SteamVR Interaction System for Unity (SteamVR haptic racks: air/empty  $\rightarrow$  [64 pulses, each 1ms], plastic/half-filled  $\rightarrow$  [128 pulses, each 2.5ms], rocks/full  $\rightarrow$  [256 pulses, each 4ms]). The visual-haptic feedback combination represents the independent variable.

After each interaction, participants were asked about the resistance (*Ratchet*) or weight (*Wagon*) experienced during interaction on a 1-to-7 Likert scale (1 = very low resistance / very lightweight; 7 = very high resistance / very heavy). When completing a scenario with a haptic feedback technique, participants also rated the haptic realism (1 = not at all realistic; 7 = highly realistic). Perceived resistance, weight, and haptic realism represent the dependent variables.

For the *Ratchet* (R) and *Wagon* (W) scenarios, we tested for each haptic technique (DPHF, PHF, VIVE) the hypothesis:

$\rightarrow$  **H-*<Scenario>-Haptic Technique>***: Users perceive different resistances/weights of the ratchets/wagons.

We further hypothesized for both scenarios:

$\rightarrow$  **H-*<Scenario>-Range>***: The range of resistances/weights conveyed with DPHF is greater than with PHF and VIVE.

$\rightarrow$  **H-*<Scenario>-Realism>***: Users perceive the DPHF rendering of resistances/weights as more realistic than PHF and VIVE.

## Part 2 – Findings

We applied the same test procedures as in part 1 to investigate our hypotheses.

**Results.** Friedman tests showed perceived resistance and weight to vary significantly 1) with the visual-haptic impression of the ratchets and wagons for DPHF (both  $p < .001$ ), PHF (both  $p \leq .036$ ) and VIVE (both  $p \leq .007$ ); and 2) with the haptic technique for air/empty, plastic/half-filled and rocks/full (all  $p < .001$ ). Significant results of the pairwise comparisons are indicated in Figure 10 presenting the results of both scenarios. The rightmost chart in Figure 9 depicts a comparison of the haptic realism of the different feedback techniques. Friedman tests also found a significant effect of feedback technique on haptic realism and range of feedback provided (Figure 10) for *Ratchet* and *Wagon* (all  $p < .001$ ).



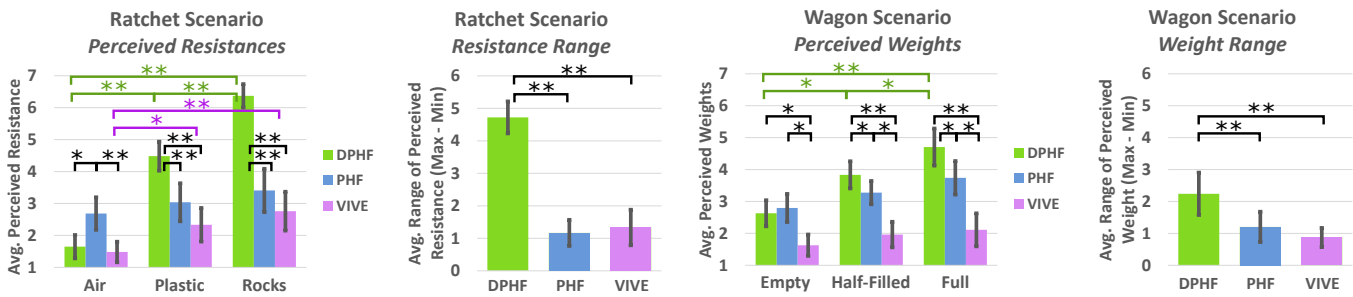


**Figure 10: Left (2 charts): Perceived *Ratchet* resistances and ranges. Right (2 charts): Perceived *Wagon* weights and ranges. Brackets indicate pairwise significant differences ( $p < .05$  (\*);  $p < .01$  (\*\*)). Error bars show 95% confidence intervals.**

*Discussion.* *Drag:on's* DPHF could render distinguishable levels of resistance and weight, confirming hypotheses **H- $\{R,W\}$ -DPHF**. The corresponding ranges rendered by DPHF were significantly greater than those of PHF and VIVE, confirming also **H- $\{R,W\}$ -Range**. Moreover, the haptic realism of DPHF was significantly higher than of PHF and VIVE when rendering ratchet resistances, corroborating **H-R-Realism**. As PHF was not found to convey significantly different resistances, nor weights, and as VIVE did not yield significantly different sensations of weight, **H- $\{R,W\}$ -PHF** and **H-W-VIVE** were not supported by our results. For VIVE, ratchet resistances of air differed significantly from those of plastic and rocks. However, the difference between plastic and rocks could not be communicated with the VIVE technique, which delivered a significantly smaller range of resistances than DPHF. **H-R-VIVE** was thus only partially confirmed. The same applies to **H-W-Realism** as in *Wagon*, the perceived realism of DPHF and PHF did not differ significantly.

From the results we conclude that mainly low resistances and weights were perceived with VIVE. PHF provided slightly higher resistances and weights, but due to its passive nature did not adapt to different materials or fill states. Different perceptions across PHF, although not significant, were likely caused by the visualization. In contrast, with DPHF, significantly different resistances and weights could be rendered, which significantly increased the haptic realism of the VR experiences compared to using standard VR controllers.

### Post-Study Results & User Feedback

Post-study SUS counts ( $M = 1.78$ ,  $SD = 1.47$ ) and means ( $M = 4.47$ ,  $SD = .85$ ) verified the general immersiveness of the VE. In the post-study questionnaire, we also asked if participants felt sick during their time in the VE (1 = not at all; 7 = I felt very sick). The post-study sickness ratings confirmed the absence of sickness issues ( $M = 1.33$ ,  $SD = .58$ ).

In debriefing, participants described *Drag:on* and its feedback as varied, suitable for many different applications, comfortable, and “feel[ing] much more real than the standard controllers”. When introduced to the concept and prototype,

some participants were surprised about how the controller looked and how it worked, and stated that they did not expect it to leverage air resistance.

## 5 DISCUSSION, LIMITATIONS & FUTURE WORK

We condense our findings, observations and experiences into a set of basic recommendations for drag and inertia-based haptic VR controllers such as *Drag:on*.

### Recommendations

- (1) To convey haptic impressions, interactions should be designed so as to cause controller movements.
- (2) To minimize real-virtual discrepancy, virtual objects should align with the fan plane (i.e. so that the plane through their largest surface area coincides with the plane parallel to the fans through the controller).
- (3) When moved, controller states with
  - min. surface area  $A$  and low rotational inertia  $I_{roll}$  (e.g.  $S_{closed}$ ) are suitable to render *small*, *lightweight*, or *empty* objects, or *low mechanical resistances*.
  - max.  $A$  and high  $I_{roll}$  (e.g.  $S_{full}$ ) are suitable to render *large*, *heavy*, or *filled* objects, or *high resistances*.
  - intermediate  $A$  and  $I_{roll}$  (e.g.  $S_{half}$ ) can render *intermediate states of size*, *heaviness*, *filling* or *resistance*.
  - asymmetric drag properties (like  $S_{left}$ ,  $S_{right}$ ) are suitable to render *relative differences in resistance*, resulting in torque felt while swinging the controller.
  - symmetric drag properties (like  $S_{closed}$ ,  $S_{half}$ ,  $S_{full}$ ) can be used in contrast to asymmetric states to render the *absence of relative differences*.
- (4) *Rotational movements* (Figure 2 a) are suitable to convey a *broad range of resistances*, and *high absolute resistances*, as drag and inertial feedback act in concert.
- (5) *Translational movements* (Figure 2 b) are suitable to convey *relations of resistance* through torque and *low absolute resistances*.

## Potential Application Areas

Besides the investigated VR interactions, we believe the haptics of *Drag:on* can enhance many more VR scenarios. As also suggested by our participants, we imagine *Drag:on* to enhance the realism of VR sport experiences (e.g. curling, racket sports or golf), and other physical interactions like rowing, swimming or diving in VR. Its feedback might also suit to simulate the resistances felt when handling tools like screwdrivers, hammers or axes, or resistances expected during everyday interactions like stirring a pot. Besides realistic scenarios, *Drag:on* could also enhance the feel of unrealistic VEs. In games, different device states could render the feel of swords or the dense atmospheres of distant planets. Holding a *Drag:on* controller in each hand, participants also suggested to simulate the feeling of being a flying bird. In a commercial controller design, we imagine the user to mount custom fans and weights that either ship with the application, or can be self-fabricated, optimizing the experience.

## Limitations & Future Work

*Drag:on* only provides distinguishable haptic impressions when moved by the user. In our study, participants were instructed to move *Drag:on* naturally as in an actual application. Even though we observed different speeds, our results show that natural interactions suffice to perceive the desired effects. It is noteworthy that these encouraging results were obtained although the feedback curve of *Drag:on* did not match every resistance profile that would have been encountered in reality. In any case, however, it is advisable to keep the velocity dependence of the feedback in mind when designing corresponding VR interactions.

A mechanical limitation of our device is *Drag:on*'s fixed orientation of the fan plane. When moving the controller parallel to this plane, the drag effect vanishes. While this leads to realistic feedback for rather flat objects, it might be unrealistic for other shapes. This can, however, be improved in future device iterations by adding an actuator to rotate the top end of the controller. The fans could thereby rotate dynamically around the roll-axis of the device to optimize their angle of attack. Integrating such an actuator would additionally enable decoupling the drag felt when swinging from the resistance felt when rotating. Using a motor to compensate for rotations of the device about its roll-axis, resistance could be felt only during translational movements. Vice versa, the fan plane could be rotated to always coincide with the translation direction to convey resistance only when rolling the device.

Other limitations of our prototype include its relatively high weight, audible and vibrotactile noise as a byproduct of the transformation, and the physical space requirements (e.g. when used in small rooms or during bi-manual interaction).

Beyond that, users can perceive the airflow during certain interactions and might perceive the weight imbalance of certain device states. Moreover, its transformation time of 570ms might still be too slow for some VR interactions. Most of these limitations, however, can be addressed in future device iterations, e.g. considering alternative form factors (e.g. origami [15]) or device designs that adapt drag independent from inertia (e.g. variable fan perforation), or by using lighter materials, faster motors, dampening, or optimized size-to-weight ratios. Beyond that, more advanced fan control could dynamically adjust the device size for collision avoidance, or compensate for velocity disparities between different users.

Besides exploring design improvements, in future research, we plan to study the impact of drag and inertia in more detail to better understand their individual contribution to the effects. It might also be worth to investigate aerodynamic lift. Further research in this direction could eventually lead to a formal model of *Drag:on*'s haptic feedback.

## 6 CONCLUSION

We presented *Drag:on*, a novel haptic VR controller providing kinesthetic sensations to VEs. *Drag:on* dynamically resizes its surface area to leverage the airflow occurring at the controller during interaction and to adapt its rotational inertia. We introduced the concept of dynamic passive haptic feedback based on drag and weight shift, and presented an implementation characterized by the sole use of low-cost and 3D-printed parts. In a user study, we explored rotational and translational controller movements and showed that *Drag:on* delivers distinguishable levels of haptic feedback. We demonstrated that the device provides suitable haptic feedback for virtual objects differing in scale or material, and even for perceiving relative differences in the strength of virtual gas streams. *Drag:on* further improved the perception of resistances felt when turning virtual ratchets and of the weight felt when moving virtual wagons, which significantly increased the haptic realism compared to standard VR controllers. We compiled our findings and observations in a set of basic recommendations for drag and weight-shift-based controllers such as *Drag:on*. Our results encourage future research to uncover the full potential of haptic feedback for VR based on air resistance and weight shift.

## ACKNOWLEDGMENTS

We thank Akhmajon Makhsadov and Sören Klingner for the programming support, David Lieberman for video shoot support, and our colleagues at DFKI & Saarland University for valuable discussions. This research was funded in part by the German Federal Ministry of Education and Research (BMBF) under grant number 01IS17043 (project ViRUX).

## REFERENCES

- [1] Jason Alexander, Anne Roudaut, Jürgen Steimle, Kasper Hornbæk, Miguel Bruns Alonso, Sean Follmer, and Timothy Merriitt. 2018. Grand Challenges in Shape-Changing Interface Research. In *Proc. CHI (CHI '18)*. ACM, New York, NY, USA, Article 299, 14 pages. <https://doi.org/10.1145/3173574.3173873>
- [2] Bruno Araujo, Ricardo Jota, Varun Perumal, Jia Xian Yao, Karan Singh, and Daniel Wigdor. 2016. Snake Charmer: Physically Enabling Virtual Objects. In *Proc. TEI (TEI '16)*. ACM, New York, NY, USA, 218–226. <https://doi.org/10.1145/2839462.2839484>
- [3] Mahdi Azmandian, Mark Hancock, Hrvoje Benko, Eyal Ofek, and Andrew D. Wilson. 2016. Haptic Retargeting: Dynamic Repurposing of Passive Haptics for Enhanced Virtual Reality Experiences. In *Proc. CHI (CHI '16)*. ACM, New York, NY, USA, 1968–1979. <https://doi.org/10.1145/2858036.2858226>
- [4] Hrvoje Benko, Christian Holz, Mike Sinclair, and Eyal Ofek. 2016. NormalTouch and TextureTouch: High-fidelity 3D Haptic Shape Rendering on Handheld Virtual Reality Controllers. In *Proc. UIST (UIST '16)*. ACM, New York, NY, USA, 717–728. <https://doi.org/10.1145/2984511.2984526>
- [5] Mourad Bouzit, George Popescu, Grigore Burdea, and Rares Boian. 2002. The Rutgers Master II-ND Force Feedback Glove. In *Proc. HAPTICS*. IEEE Computer Society, 145–152. <https://doi.org/10.1109/HAPTICS.2002.998952>
- [6] Lung-Pan Cheng, Li Chang, Sebastian Marwecki, and Patrick Baudisch. 2018. iTurk: Turning Passive Haptics into Active Haptics by Making Users Reconfigure Props in Virtual Reality. In *Proc. CHI (CHI '18)*. ACM, New York, NY, USA, Article 89, 10 pages. <https://doi.org/10.1145/3173574.3173663>
- [7] Lung-Pan Cheng, Patrick Lühne, Pedro Lopes, Christoph Sterz, and Patrick Baudisch. 2014. Haptic Turk: A Motion Platform Based on People. In *Proc. CHI (CHI '14)*. ACM, New York, NY, USA, 3463–3472. <https://doi.org/10.1145/2556288.2557101>
- [8] Lung-Pan Cheng, Eyal Ofek, Christian Holz, Hrvoje Benko, and Andrew D. Wilson. 2017. Sparse Haptic Proxy: Touch Feedback in Virtual Environments Using a General Passive Prop. In *Proc. CHI (CHI '17)*. ACM, New York, NY, USA, 3718–3728. <https://doi.org/10.1145/3025453.3025753>
- [9] Lung-Pan Cheng, Thijs Roumen, Hannes Rantzsch, Sven Köhler, Patrick Schmidt, Robert Kovacs, Johannes Jasper, Jonas Kemper, and Patrick Baudisch. 2015. TurkDeck: Physical Virtual Reality Based on People. In *Proc. UIST (UIST '15)*. ACM, New York, NY, USA, 417–426. <https://doi.org/10.1145/2807442.2807463>
- [10] Inrak Choi, Heather Culbertson, Mark R. Miller, Alex Olwal, and Sean Follmer. 2017. Gravity: A Wearable Haptic Interface for Simulating Weight and Grasping in Virtual Reality. In *Proc. UIST (UIST '17)*. ACM, New York, NY, USA, 119–130. <https://doi.org/10.1145/3126594.3126599>
- [11] Inrak Choi and Sean Follmer. 2016. Wolverine: A Wearable Haptic Interface for Grasping in VR. In *Adjunct Proc. UIST (UIST '16 Adjunct)*. ACM, New York, NY, USA, 117–119. <https://doi.org/10.1145/2984751.2985725>
- [12] Inrak Choi, Eyal Ofek, Hrvoje Benko, Mike Sinclair, and Christian Holz. 2018. CLAW: A Multifunctional Handheld Haptic Controller for Grasping, Touching, and Triggering in Virtual Reality. In *Proc. CHI (CHI '18)*. ACM, New York, NY, USA, Article 654, 13 pages. <https://doi.org/10.1145/3173574.3174228>
- [13] HTC Corporation. 2018. HTC Vive Virtual Reality System. <https://www.vive.com/> Retrieved Aug 29, 2018.
- [14] Lionel Dominjon, Anatole Lécuyer, Jean-Marie Burkhardt, Paul Richard, and Simon Richir. 2005. Influence of Control/Display Ratio on the Perception of Mass of Manipulated Objects in Virtual Environments. In *Proc. VR*. IEEE Computer Society, 19–25. <https://doi.org/10.1109/VR.2005.1492749>
- [15] Alexandra Fuchs, Miriam Sturdee, and Johannes Schöning. 2018. Fold-Watch: Using Origami-inspired Paper Prototypes to Explore the Extension of Output Space in Smartwatches. In *Proc. NordiCHI (NordiCHI '18)*. ACM, New York, NY, USA, 47–59. <https://doi.org/10.1145/3240167.3240173>
- [16] Eisuke Fujinawa, Shigeo Yoshida, Yuki Koyama, Takuji Narumi, Tomohiro Tanikawa, and Michitaka Hirose. 2017. Computational Design of Hand-held VR Controllers Using Haptic Shape Illusion. In *Proc. VRST (VRST '17)*. ACM, New York, NY, USA, Article 28, 10 pages. <https://doi.org/10.1145/3139131.3139160>
- [17] James J. Gibson. 1933. Adaptation, After-effect and Contrast in the Perception of Curved Lines. *Journal of Experimental Psychology* 16, 1 (1933), 1–31. <https://doi.org/10.1037/h0074626>
- [18] Xiaochi Gu, Yifei Zhang, Weize Sun, Yuanzhe Bian, Dao Zhou, and Per Ola Kristensson. 2016. Dexmo: An Inexpensive and Lightweight Mechanical Exoskeleton for Motion Capture and Force Feedback in VR. In *Proc. CHI (CHI '16)*. ACM, New York, NY, USA, 1991–1995. <https://doi.org/10.1145/2858036.2858487>
- [19] Seongkook Heo, Christina Chung, Geehyuk Lee, and Daniel Wigdor. 2018. Thor's Hammer: An Ungrounded Force Feedback Device Utilizing Propeller-Induced Propulsive Force. In *Proc. CHI (CHI '18)*. ACM, New York, NY, USA, Article 525, 11 pages. <https://doi.org/10.1145/3173574.3174099>
- [20] Brent Edward Insko. 2001. *Passive Haptics Significantly Enhances Virtual Environments*. Ph.D. Dissertation. University of North Carolina at Chapel Hill, USA. <http://www.cs.unc.edu/techreports/01-017.pdf>
- [21] Seungwoo Je, Hyelip Lee, Myung Jin Kim, and Andrea Bianchi. 2018. Wind-Blaster: A Wearable Propeller-based Prototype That Provides Ungrounded Force-Feedback. In *ACM SIGGRAPH 2018 Emerging Technologies (SIGGRAPH '18)*. ACM, New York, NY, USA, Article 23, 2 pages. <https://doi.org/10.1145/3214907.3214915>
- [22] Luv Kohli. 2013. *Redirected Touching*. Ph.D. Dissertation. University of North Carolina at Chapel Hill, USA. <http://www.cs.unc.edu/techreports/13-002.pdf>
- [23] Andrey Krekhov, Katharina Emmerich, Philipp Bergmann, Sebastian Cmentowski, and Jens Krüger. 2017. Self-Transforming Controllers for Virtual Reality First Person Shooters. In *Proc. CHI PLAY (CHI PLAY '17)*. ACM, New York, NY, USA, 517–529. <https://doi.org/10.1145/3116595.3116615>
- [24] Johnny C. Lee, Scott E. Hudson, and Edward Tse. 2008. Foldable Interactive Displays. In *Proc. UIST (UIST '08)*. ACM, New York, NY, USA, 287–290. <https://doi.org/10.1145/1449715.1449763>
- [25] Pedro Lopes, Alexandra Ion, and Patrick Baudisch. 2015. Impacto: Simulating Physical Impact by Combining Tactile Stimulation with Electrical Muscle Stimulation. In *Proc. UIST (UIST '15)*. ACM, New York, NY, USA, 11–19. <https://doi.org/10.1145/2807442.2807443>
- [26] Pedro Lopes, Sijing You, Lung-Pan Cheng, Sebastian Marwecki, and Patrick Baudisch. 2017. Providing Haptics to Walls & Heavy Objects in Virtual Reality by Means of Electrical Muscle Stimulation. In *Proc. CHI (CHI '17)*. ACM, New York, NY, USA, 1471–1482. <https://doi.org/10.1145/3025453.3025600>
- [27] Thomas H. Massie and J. Kenneth Salisbury. 1994. The PHANTOM Haptic Interface: A Device for Probing Virtual Objects. In *Proc. ASME Dynamic Systems and Control Division*. 295–301.
- [28] William A. McNeely. 1993. Robotic Graphics: A New Approach to Force Feedback for Virtual Reality. In *Proc. VRAIS*. IEEE Computer Society, 336–341. <https://doi.org/10.1109/VRAIS.1993.380761>
- [29] William R. Provancher. 2014. Creating Greater VR Immersion by Emulating Force Feedback with Ungrounded Tactile Feedback. *IQT Quarterly* 6, 2 (2014), 18–21. [http://tacticalhaptics.com/wp-content/uploads/2013/10/IQT\\_Quarterly\\_Fall\\_2014\\_Provancher-Final.pdf](http://tacticalhaptics.com/wp-content/uploads/2013/10/IQT_Quarterly_Fall_2014_Provancher-Final.pdf)



- [30] Michael Rietzler, Florian Geiselhart, Jan Gugenheimer, and Enrico Rukzio. 2018. Breaking the Tracking: Enabling Weight Perception Using Perceivable Tracking Offsets. In *Proc. CHI (CHI '18)*. ACM, New York, NY, USA, Article 128, 12 pages. <https://doi.org/10.1145/3173574.3173702>
- [31] Michael Rietzler, Katrin Plaumann, Taras Kränzle, Marcel Erath, Alexander Stahl, and Enrico Rukzio. 2017. VaiR: Simulating 3D Airflows in Virtual Reality. In *Proc. CHI (CHI '17)*. ACM, New York, NY, USA, 5669–5677. <https://doi.org/10.1145/3025453.3026009>
- [32] Joseph M. Romano and Katherine J. Kuchenbecker. 2009. The AirWand: Design and Characterization of a Large-Workspace Haptic Device. In *2009 IEEE International Conference on Robotics and Automation*. 1461–1466. <https://doi.org/10.1109/ROBOT.2009.5152339>
- [33] Tomoya Sasaki, Richard Sahala Hartanto, Kao-Hua Liu, Keitarou Tsuchiya, Atsushi Hiyama, and Masahiko Inami. 2018. LevioPole: Mid-air Haptic Interactions Using Multirotor. In *ACM SIGGRAPH 2018 Emerging Technologies (SIGGRAPH '18)*. ACM, New York, NY, USA, Article 12, 2 pages. <https://doi.org/10.1145/3214907.3214913>
- [34] Jotaro Shigeyama, Takeru Hashimoto, Shigeo Yoshida, Taiju Aoki, Takuji Narumi, Tomohiro Tanikawa, and Michitaka Hirose. 2018. Transcalibur: Dynamic 2D Haptic Shape Illusion of Virtual Object by Weight Moving VR Controller. In *ACM SIGGRAPH 2018 Posters (SIGGRAPH '18)*. ACM, New York, NY, USA, Article 29, 2 pages. <https://doi.org/10.1145/3230744.3230804>
- [35] Adalberto L. Simeone, Eduardo Velloso, and Hans Gellersen. 2015. Substitutional Reality: Using the Physical Environment to Design Virtual Reality Experiences. In *Proc. CHI (CHI '15)*. ACM, New York, NY, USA, 3307–3316. <https://doi.org/10.1145/2702123.2702389>
- [36] Alexa F. Siu, Eric J. Gonzalez, Shenli Yuan, Jason B. Ginsberg, and Sean Follmer. 2018. shapeShift: 2D Spatial Manipulation and Self-Actuation of Tabletop Shape Displays for Tangible and Haptic Interaction. In *Proc. CHI (CHI '18)*. ACM, New York, NY, USA, Article 291, 13 pages. <https://doi.org/10.1145/3173574.3173865>
- [37] Mel Slater, Martin Usoh, and Anthony Steed. 1994. Depth of Presence in Virtual Environments. *Presence: Teleoperators and Virtual Environments* 3, 2 (1994), 130–144. <https://doi.org/10.1162/pres.1994.3.2.130>
- [38] Rajinder Sodhi, Ivan Poupyrev, Matthew Glisson, and Ali Israr. 2013. AIREAL: Interactive Tactile Experiences in Free Air. *ACM Trans. Graph.* 32, 4, Article 134 (July 2013), 10 pages. <https://doi.org/10.1145/2461912.2462007>
- [39] Mandayam A. Srinivasan and Cagatay Basdogan. 1997. Haptics in Virtual Environments: Taxonomy, Research Status, and Challenges. *Computers & Graphics* 21, 4 (1997), 393–404. [https://doi.org/10.1016/S0097-8493\(97\)00030-7](https://doi.org/10.1016/S0097-8493(97)00030-7)
- [40] Evan Strasnick, Christian Holz, Eyal Ofek, Mike Sinclair, and Hrvoje Benko. 2018. Haptic Links: Bimanual Haptics for Virtual Reality Using Variable Stiffness Actuation. In *Proc. CHI (CHI '18)*. ACM, New York, NY, USA, Article 644, 12 pages. <https://doi.org/10.1145/3173574.3174218>
- [41] Yuriko Suzuki and Minoru Kobayashi. 2005. Air Jet Driven Force Feedback in Virtual Reality. *IEEE Computer Graphics and Applications* 25, 1 (Jan 2005), 44–47. <https://doi.org/10.1109/MCG.2005.1>
- [42] Yuriko Suzuki, Minoru Kobayashi, and Satoshi Ishibashi. 2002. Design of Force Feedback Utilizing Air Pressure Toward Untethered Human Interface. In *CHI '02 Extended Abstracts on Human Factors in Computing Systems (CHI EA '02)*. ACM, New York, NY, USA, 808–809. <https://doi.org/10.1145/506443.506608>
- [43] Susumu Tachi, Taro Maeda, Ryokichi Hirata, and Hiroshi Hoshino. 1994. A Construction Method of Virtual Haptic Space. In *Proc. ICAT*. 131–138. <http://icat.vrsj.org/papers/94131.pdf>
- [44] Richard Q. Van der Linde, Piet Lammertse, Erwin Frederiksen, and B. Ruiters. 2002. The HapticMaster, a New High-Performance Haptic Interface. In *Proc. Eurohaptics*. 1–5.
- [45] Eric Whitmire, Hrvoje Benko, Christian Holz, Eyal Ofek, and Mike Sinclair. 2018. Haptic Revolver: Touch, Shear, Texture, and Shape Rendering on a Reconfigurable Virtual Reality Controller. In *Proc. CHI (CHI '18)*. ACM, New York, NY, USA, Article 86, 12 pages. <https://doi.org/10.1145/3173574.3173660>
- [46] E. J. Williams. 1949. Experimental Designs Balanced for the Estimation of Residual Effects of Treatments. *Australian Journal of Chemistry* 2, 2 (1949), 149–168. <https://doi.org/10.1071/CH9490149>
- [47] André Zenner and Antonio Krüger. 2017. Shifty: A Weight-Shifting Dynamic Passive Haptic Proxy to Enhance Object Perception in Virtual Reality. *IEEE Transactions on Visualization and Computer Graphics* 23, 4 (2017), 1285–1294. <https://doi.org/10.1109/TVCG.2017.2656978>